*Desalination and Water Treatment*
www.deswater.com

doi: 10.5004/dwt.2020.26261

204 (2020) 377–387
November

# Effective glyphosate degradation through the combination of ozone/hydrogen peroxide oxidation and coagulation

Lei Chen[a,*], Shengbao Zhou[b], Yanhua Xu[a], Yongjun Sun[b,*], Huaili Zheng[c]

[a]*Jiangsu Key Laboratory of Industrial Water-Conservation and Emission Reduction, College of Environment, Nanjing Tech University, Nanjing 211800, China, email: matlabvisual@163.com (L. Chen)*
[b]*College of Urban Construction, Nanjing Tech University, Nanjing 211800, China, email: sunyongjun@njtech.edu.cn (Y. Sun)*
[c]*Key Laboratory of the Three Gorges Reservoir Region's Eco-Environment, State Ministry of Education, Chongqing University, Chongqing 400045, China*

Received 7 March 2020; Accepted 13 June 2020

## ABSTRACT

Phosphorus removal from glyphosate wastewater is a common problem that requires an urgent solution. In this study, ozone-catalyzed oxidation coupled with coagulation is used to treat glyphosate-simulated wastewater. The effect of ozone dosage, hydrogen peroxide, pH, reaction time, and amount of catalyst on the efficiency of glyphosate removal, color, biological toxicity, total phosphorus, organic phosphorus, and inorganic phosphorus are studied in ozone-catalyzed oxidation. Afterward, the effect of coagulant species, pH, dosage, stirring rate, stirring time, and water temperature on the efficiency of glyphosate removal, total phosphorus, organic phosphorus, and inorganic phosphorus by coagulation process are also investigated. The removal rates of glyphosate and chroma reach 56.97% and 93.75%, respectively, at the optimal conditions of ozone-catalyzed oxidation, and the biological toxicity of wastewater changes from high to low. Ozone-catalyzed oxidation can effectively reduce color and wastewater biological toxicity. After the ozone-catalyzed coupled coagulation treatment, the removal rates of glyphosate, total phosphorus, organic phosphorus, and inorganic phosphorus by the coagulation process reach 71.13%, 93.75%, 90.48%, and 96.3%, respectively, at optimal conditions. This study demonstrates the effectiveness and superiority of ozone-catalyzed oxidation and coagulation coupling for glyphosate degradation.

*Keywords:* Glyphosate; Ozone-catalytic oxidation; Coagulation; Combination process

## 1. Introduction

Developed to replace organochlorine pesticides, organophosphorus pesticides are now widely used in various countries worldwide due to their advantages, such as high efficacy, low harm, and low residual toxicity [1]. The heavy use of glyphosate considerably promotes agricultural development, but its residues cause increasing environmental pollution that has generated widespread concern [2]. Different levels of resulting pollution to water sources, soil, air, and ecosystems lead to the necessity of urgently determining how to treat glyphosate-containing wastewater efficiently and cost-effectively [3].

Various wastewater treatment processes are gradually developed to reduce glyphosate concentration in water environment and reduce its damage to natural ecosystems and human health [4]. Traditional glyphosate wastewater treatment mainly uses the strong oxidation of Fenton reagent to degrade glyphosate [5]. The Fenton method can oxidize toxic and harmful substances in wastewater into small molecules or inorganic substances, reducing the difficulty for subsequent processing [6]. However, the Fenton

---

* Corresponding authors.

reaction process requires a large amount of reagents such as acid, alkali, and hydrogen peroxide. In addition, the reaction produces an iron sludge that is a hazardous waste, which substantially increases the wastewater treatment operation cost of pesticide companies [7]. As an alternative to the Fenton method, ozone-based advanced oxidation technology has attracted research attention due to its good oxidation effect, safety, and absence of residue. Exploring an easy-to-operate and highly practical ozone oxidation system has far-reaching significance for actual organic phosphorus wastewater treatment [8]. At present, $H_2O_2/O_3$ is a widely used system in ozone-based advanced oxidation technology. The system has satisfactory removal of organic matter under alkaline conditions [9]. However, under acidic water body conditions, $H_2O_2$ is difficult to deprotonate and cannot effectively stimulate ozone to generate hydroxyl radicals [10]. As such, the degradation efficiency of organic matter decreases. Therefore, the use of metal catalysts can improve the efficiency of $H_2O_2/O_3$ system degradation of organic matter. Simultaneously, the reaction mode of hydrogen peroxide and ozone is shown in Eqs. (1)–(5) [11,12].

$$O_2 + 2H + 2e^- \rightarrow H_2O_2 \tag{1}$$

$$2O_3 + 2HO_2^- + +H_2O \rightarrow 2HO^\bullet + 3O_2 + OH^- + HO_2^{-\bullet} \tag{2}$$

$$O_3 + 2e^- \rightarrow O_3^{\bullet -} \tag{3}$$

$$O_3^{\bullet -} + H_2O \rightarrow HO^{\cdot} + O_2 + HO^- \tag{4}$$

$$H_2O_2 + O_{23} + h\upsilon \rightarrow 2HO^\bullet + H_2O \tag{5}$$

The largest problem in glyphosate wastewater treatment is how to convert more organic phosphorus into orthophosphate and from there, remove the inorganic phosphorus using chemical precipitation [13,14]. Therefore, this study investigates the applicability and effectiveness of ozone-catalyzed coupled coagulation in the pretreatment of glyphosate wastewater. First, the strong oxidizing property of hydroxyl radicals generated by ozone oxidizes the organic phosphorus in glyphosate to an inorganic phosphorus (phosphate) form that is easily coagulated and precipitated by a coagulant [15,16]. The larger flocculent precipitate is formed by coagulation, and can improve sedimentation to effectively remove the phosphorus in wastewater. In this thesis, various factors affecting the optimal treatment of ozone-catalyzed oxidation coupled coagulation to treat glyphosate wastewater are studied [17]. We hope that the findings can be used to treat glyphosate wastewater through ozone-catalytic oxidation coupled coagulation and provide certain technical references. Moreover, a method that can quickly pretreat high glyphosate wastewater is desirable to address the shortcomings of the existing technology while improving the efficiency of wastewater treatment [18]. For example, the single ozone oxidation method has low removal efficiency of total phosphorus, and coagulation cannot effectively remove organic phosphorus and matter [19].

This experiment first studies the effects of ozone dosage, hydrogen peroxide dosage, pH, reaction time, and catalyst ratio on the catalytic oxidation of ozone to remove glyphosate, color, and biological toxicity from simulated wastewater. The effects of ozone-catalyzed oxidation and coagulation–precipitation coupling on the removal of glyphosate, chroma, and biological toxicity are discussed. The initial pH, reaction temperature, coagulant concentration, coagulant dosage, coagulant type, stirring time, and stirring rate are studied to remove glyphosate, total phosphorus, organic phosphorus, inorganic phosphorus, and biological toxicity. During the reaction, the changes in the spectral characteristics of water samples are analyzed.

## 2. Materials and methods

### *2.1. Materials*

Chromatographically pure *n*-hexane and analytical grade potassium persulfate, ascorbic acid, ammonium molybdate, silver sulfate, ferrous ammonium sulfate, potassium dichromate, concentrated sulfuric acid, anhydrous sodium sulfate, 4-aminoantipyroline, ammonium chloride, ammonia, potassium ferricyanide, polyaluminum chloride, polyaluminum sulfate, polysulfuric acid iron, polyferric chloride, polyaluminum ferric sulfate, polyaluminum ferric chloride, and polyammonium polyacrylate were purchased from Sinopharm Shanghai Chemical Reagent Company, China. The glyphosate isopropylamine salt content, purchased from Weifang Aofeng Crop Disease Control Co., Ltd. (China), was 41%. Ozone catalyst was prepared in this laboratory, and the work about preparation and characterization were shown in our previous paper [17]. The ozone catalyst used in this study was Fe-Co@$Al_2O_3$. The iron and cobalt of ferric chloride and cobalt nitrate were loaded on the surface of activated alumina microspheres by gel–sol impregnation method, and the ozone catalyst Fe-Co@$Al_2O_3$ under the condition of calcination at 550°C in a muffle furnace was obtained. In this experiment, the glyphosate-simulated wastewater selected was light blue and transparent, with a slightly pungent odor, concentration of 33.4 mg/L, and pH of 7.1.

### *2.2. Experiments*

An ozone generator (CF-G-3-010g, Qingdao Guolin Company, Qingdao, China) and an ozone detector (ozone detector, LontecLT-200B, Qingdao Langke Electronic Technology Co., Ltd., Qingdao, China) were used in the preparation of $O_2/O_3$ mixed gas. The mixed gas was passed into a self-made plexiglass reactor placed in an electric heating thermostatic water bath, and a certain amount of catalyst was weighed. Using the same electronic balance, a certain amount of coagulant was weighed, then a certain amount of distilled water was added and stirred with a temperature-controlled magnetic stirrer for 10 min to obtain a coagulant solution. The peristaltic pump was used to recycle the wastewater in the $O_3$ reactor. Under optimal reaction conditions of ozone-catalyzed oxidation, the effect of coagulation and sedimentation on the glyphosate wastewater treatment was studied through single-factor optimization experiments. The types of coagulant, coagulant dosage, coagulant concentration, initial effects of pH, stirring rate, stirring time, and reaction temperature on the removal rate of glyphosate, total phosphorus, organic phosphorus, inorganic phosphorus, and biological toxicity in solution are likewise studied. Dilution multiple methods were used to measure the chromaticity of wastewater and the safety rapid detector (BHP9514, Beijing Hamamatsu, China) for drinking water was used to determine the luminous rate of water samples relative to pure water. Potassium persulfate was used for high-temperature digestion and oxidation, and ammonium molybdate spectrophotometry (GB11893-1989) through an ultraviolet spectrophotometer (UV2600, Shimadzu Corporation, Japan) was used to determine the total phosphorus (TP) concentration in water samples at 700 nm. Phosphate ($PO_4^{3-}$) concentration was measured by high-performance liquid chromatography (LC-20A, Shimadzu Corporation, Japan) to obtain the relevant conversion rule of phosphorus. Organic phosphorus was totally different from phosphate. Chroma is tested by Colorimeter (Hash LICO620 Desktop Colorimeter, HACH, USA). Chroma is an indicator for quantitative determination of the color of various treated waters, and it indirectly reflects the removal rate of colored organic matter in wastewater.

## 3. Results and discussions

### *3.1. Degradation of glyphosate by ozone-catalytic oxidation*

### *3.1.1. Effects of ozone dosage on glyphosate degradation*

Fig. 1 shows that the removal rate of glyphosate and solution color increases with ozone dosage. Toxicity decreases from the original poisoning to low toxicity. When the dosage reaches 25 mg/L, glyphosate and chroma are removed and toxicity is greatly reduced. The removal rate of glyphosate and chroma is 100.00% at 30 mg/L.

In a slow kinetic reaction system, direct and indirect ozone reactions remove glyphosate from water by competing for ozone depletion. Ozone oxidation is generally in a rapid kinetic system in the first stage [20]. Direct oxidation of ozone degrades glyphosate in wastewater, and the rates of these processes increases as the ozone concentration increases [21]. The biological toxicity of glyphosate thus decreases. In addition, glyphosate decomposition and color removal accelerates because ozone can self-decompose in water to produce a strong oxidizing hydroxyl radical ($HO^{\bullet}$) [22]. The removal rate of glyphosate is 99.09% at 25 mg/L, which is therefore the optimal ozone dosage.

### *3.1.2. Effect of hydrogen peroxide dosage on glyphosate degradation*

Fig. 2a shows that the removal rate of glyphosate and chromaticity gradually increases with increasing amount of hydrogen peroxide. When the amount of hydrogen peroxide reaches 0.20%, the removal rate of glyphosate and chroma are 74.24% and 100.00%, respectively.

In the $O_3/H_2O_2$ reaction system, strong oxidative hydroxyl radicals are generated. As the hydrogen peroxide concentration increases, the concentration of generated hydroxyl radicals and the removal rate of glyphosate increase [23]. The amount of ozone in the system is limited and when depleted, the effective components in the system decrease, and the removal efficiency reaches a bottleneck. The concentration of hydrogen peroxide may reach a critical concentration, which inhibits the reaction from proceeding [24]. Fig. 2b shows that the relative luminous rate initially increases and then decreases. In addition, the biological toxicity of the solution changes from low to poisoning, which is due to the production of more toxic substances during the reaction [25]. The removal rate of glyphosate increases with an increasing amount of hydrogen peroxide, but the solution toxicity also increases. Therefore, the optimal amount of hydrogen peroxide is 0.05‰.

### *3.1.3. Effect of pH on glyphosate degradation*

In ozone oxidation, the increase in pH can improve the removal efficiency of organic matter. Fig. 3a shows that the removal rate of glyphosate at pH = 4 is 29.09%. With the increase of pH, the removal rate of glyphosate shows a steady upward trend and reaches its peak of 40.5% at pH = 9. At this pH, biological toxicity is also at its lowest, as shown in Fig. 3b.

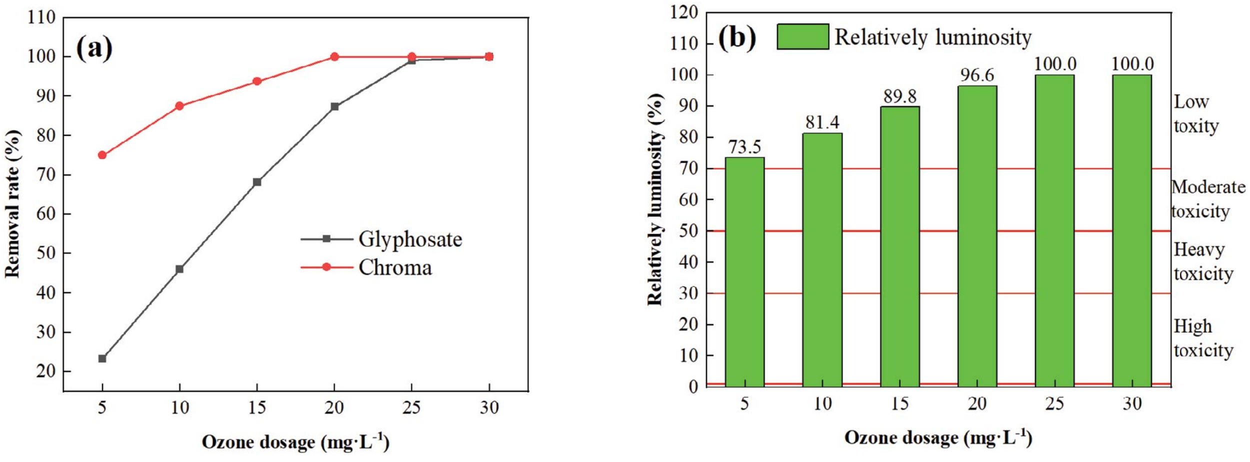

Fig. 1. Effects of ozone dosage on glyphosate degradation: (a) glyphosate and chroma removal rates and (b) relative luminosity.

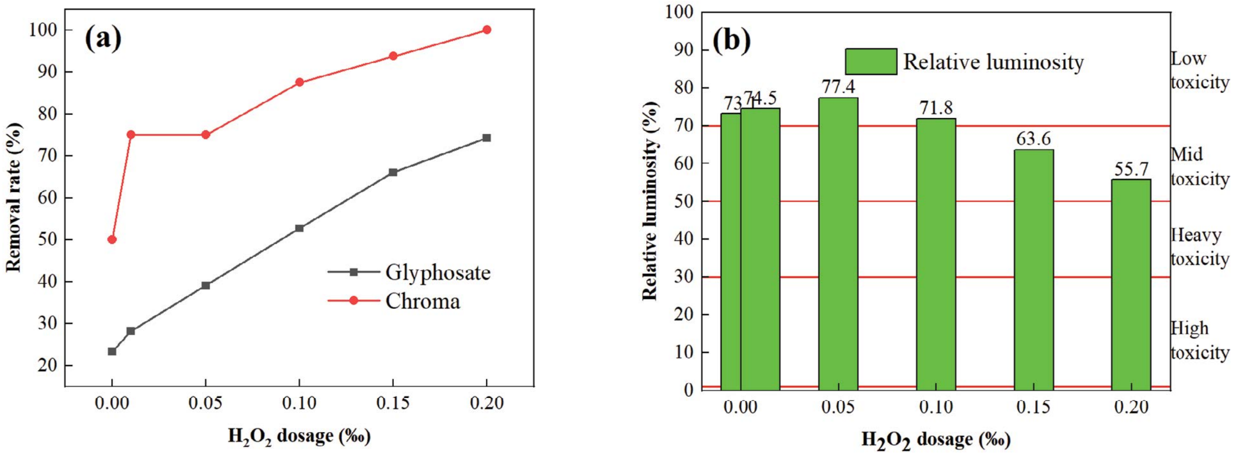

Fig. 2. Effects of hydrogen peroxide dosage on glyphosate degradation: (a) glyphosate and chroma removal rates and (b) relative luminosity.

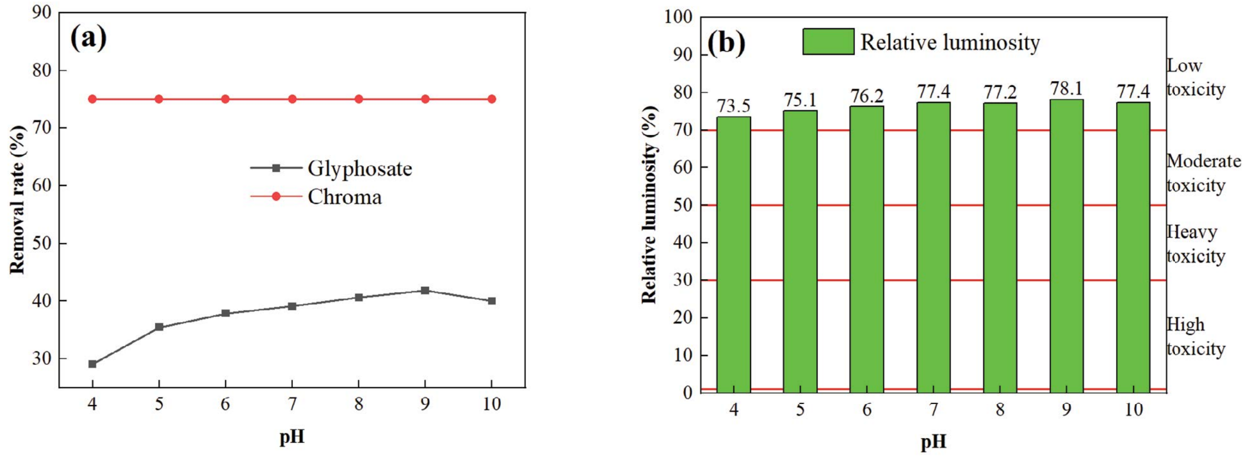

Fig. 3. Effects of pH on glyphosate degradation: (a) glyphosate and chroma removal rates and (b) relative luminosity.

In acidic conditions, protons can scavenge hydroxyl radicals and reduce removal efficiency [26,27]. Moreover, in acidic condition, protons can directly react with peroxide and produce water [28]. In the alkaline system, a large amount of OH– in the water can accelerate the hydrolysis rate of glyphosate in the solution and promote the reaction between ozone and hydrogen peroxide to generate more active hydroxyl radicals [29]. The chain reaction generates more active free radicals, accelerates the decomposition of glyphosate, and accordingly increases the removal rate of glyphosate. When the pH value continues to increase, the reaction of the hydroxyl radicals in the system weakens, leading to decreased glyphosate degradation and removal rates [30]. In a steady-state, the chroma removal rate is approximately 75%. Therefore, for the reaction, the optimum pH is 9.

### *3.1.4. Effect of reaction time on glyphosate degradation*

Fig. 4 shows that the removal and relative luminous rates of glyphosate increase with the reaction time. The removal rate of glyphosate increases from 25.2% at 5 min to 41.8% at 20 min. Then the reaction time increases but the removal rate and solution toxicity remain almost unchanged. The chroma removal rate is consistent at 75.0%.

These results can be explained as follows. The degradation rate is relatively fast in the early stages of the reaction when the concentration of dissolved ozone in the water is relatively high. Part of the ozone is involved in the reaction and therefore begins to decay and gradually decreases the degradation rate as the reaction time increases [31]. Another possibility is that during the rapid ozone reaction, glyphosate is partially mineralized to generate a large amount of carbonate/bicarbonate ions, which quenches the generated hydroxyl radicals and slows down the reaction rate [32]. Therefore, the optimal reaction time is 20 min.

### *3.1.5. Effect of catalyst radio on glyphosate degradation*

Fig. 5 shows that glyphosate degradation, chroma removal, and relative luminosity rates increase simultaneously with the increase of the catalyst ratio at ozone dosage 10 mg/L and hydrogen peroxide dosage 0.05‰. When the

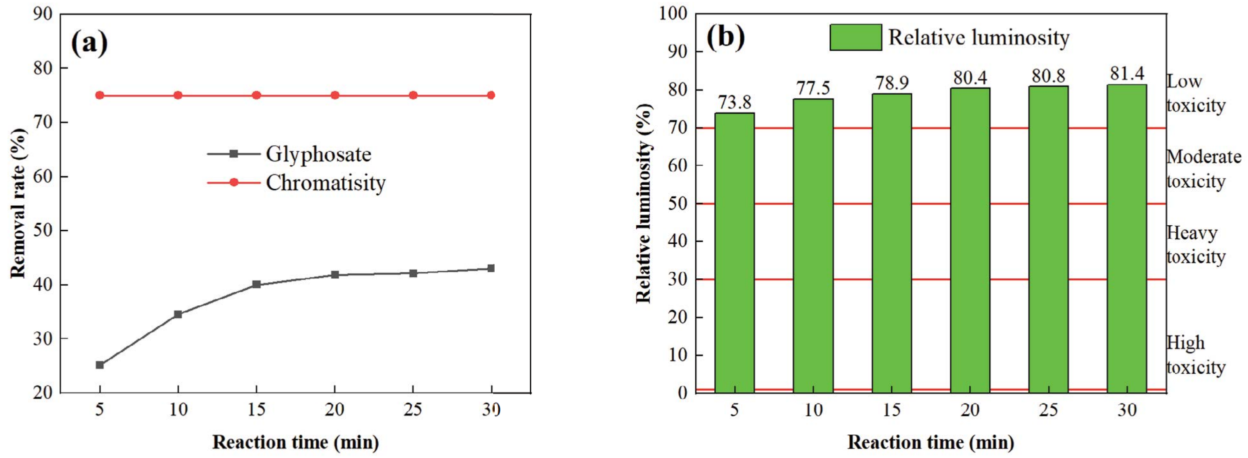

Fig. 4. Effects of reaction time on glyphosate degradation: (a) glyphosate and chroma removal rates and (b) relative luminosity.

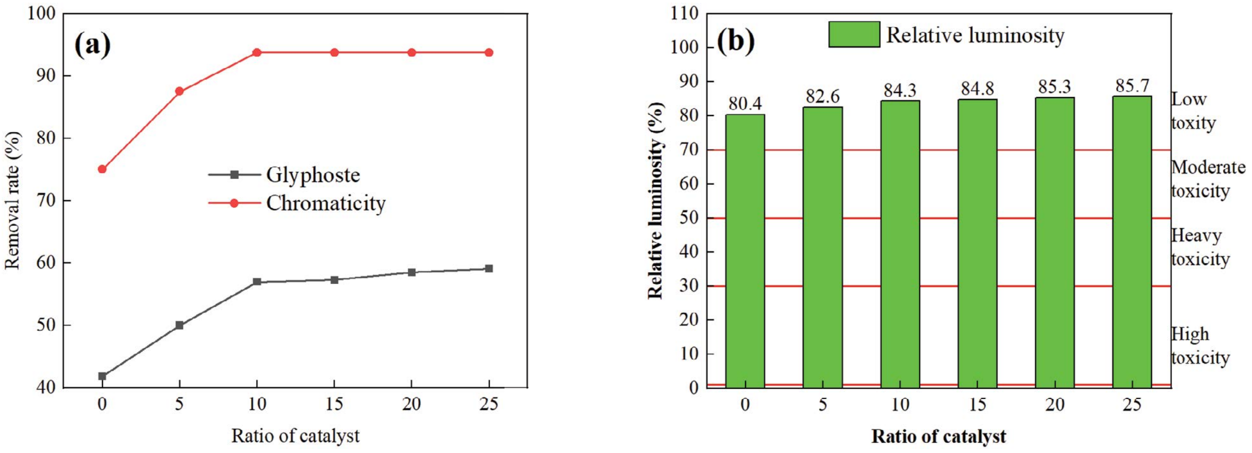

Fig. 5. Effect of catalyst dosage on glyphosate degradation: (a) glyphosate and chroma removal rates and (b) relative luminosity.

catalyst ratio is 0, the removal rates of glyphosate and chroma are 41.82% and 75%, respectively. When the ratio increases to 10, the removal rates increase to 57.27% and 93.75%, respectively. In addition, the total organic carbon removal rate is 18.9% after 30 min of ozone catalytic oxidation.

The increase of catalyst ratio provides more high-quality mesoporous structure for glyphosate adsorption and ozonation decomposition. Moreover, active surface materials can catalyze ozone to generate hydroxyl radicals, accelerating glyphosate degradation [33]. The further increase of the catalyst ratio adsorbs newly generated oxygen-containing negative ions such as $HO_2$– and $O_2^{\bullet-}$, which slow down the ozone decomposition and maintains the removal rate. Thus, the optimum catalyst ratio is 10.

### *3.2. Glyphosate degradation through combined ozone-catalytic oxidation and coagulation*

#### *3.2.1. Effect of coagulants on glyphosate removal*

Fig. 6 shows the change rules of coagulation treatment simulated water samples with different types of coagulant glyphosate, total phosphorus, organic phosphorus, inorganic phosphorus, and biological toxicity. Under the same dosage and concentration, the removal rate of calcium chloride is less than those of other types of coagulants, of which those of iron-based coagulants are high. For aluminum coagulants, the treatment effect of composite polymers is better than that of polymers, which is consistent with the findings of related research. Therefore, the best coagulant is polymeric aluminum ferric sulfate (PAFS), with removal rates for glyphosate, total phosphorus, organic phosphorus, and inorganic phosphorus at 70.83%, 47.62%, and 88.89%, respectively.

Coagulants can remove glyphosate from solutions through destabilization and adsorption bridging. The changes of total phosphorus and inorganic phosphorus are the same, but the removal of the former is larger than that of the latter because the ozone-catalyzed oxidation converts most of the phosphorus in glyphosate to phosphate inorganic phosphorus [34]. A portion of the glyphosate is decomposed into other small organic phosphorus-containing substances that can be removed by coagulation precipitation and co-precipitation. PAFS has better dephosphorization effect

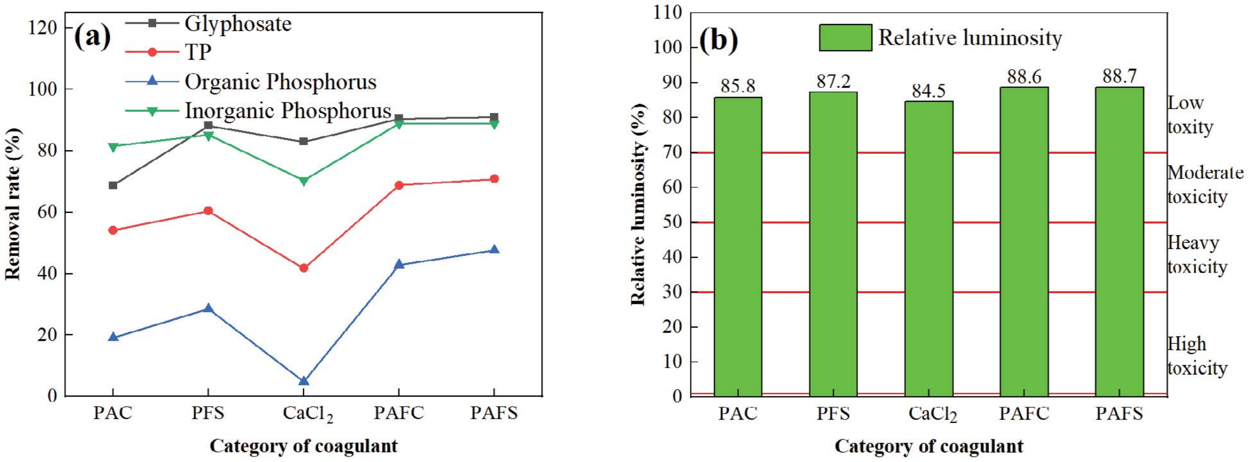

Fig. 6. Effect of coagulants on glyphosate removal: (a) glyphosate, total phosphorus, organic phosphorus, and inorganic phosphorus removal rates and (b) relative luminosity.

than other coagulants because it combines iron salt and phosphate with more stable iron phosphate precipitation and aluminum salt alum and has strong adsorption capacity. PAFS generates precipitates by phosphate reaction and high-charged aluminum-iron polynuclear complex ions or metal hydroxide gels after hydrolysis, which can produce cohesive bridge flocculation and sweeping precipitation on phosphate precipitates [35]. Phosphate precipitation is adsorbed and co-precipitated, thereby achieving thorough phosphorus removal. Additionally, the experiments of PAFS and other coagulants coagulation treatment of glyphosate wastewater are added, and the removal efficiency of glyphosate by PAFS and other coagulants is less than 20%. This shows that the soluble organic phosphorus cannot react with the iron ions (aluminum and calcium ion) in PAFS and other coagulants, and the coagulation process alone cannot effectively remove the soluble organic phosphorus.

### 3.2.2. Effect of initial wastewater pH value on glyphosate removal

Fig. 7 shows that as the initial pH increases, the removal rates of various indicators initially increase then decrease, and reach their maximum values when the pH is 6–8. When pH is 8, the removal rates of glyphosate, total phosphorus, organic phosphorus, and inorganic phosphorus are 91.41%, 72.92%, 52.38%, and 88.89%, respectively.

PAFS is a cationic coagulant and has a strong positive charge, whereas the surface of colloidal particles in domestic sewage generally has a negative charge. Both undergo strong electrical neutralization and adsorption bridging. At low pH value, an acidic solution has countless cations that are not conducive to PAFS hydrolysis [36]. The electrical neutralization and adsorption bridging of PAFS then decrease, which is not conducive to the removal of inorganic phosphorus, and the biological toxicity increases. At extremely high pH, the simulated solution is alkaline and contains more OH–, which neutralizes the positive charge of PAFS [37]. Therefore, the amount of charge carried by PAFS decreases and becomes electrically neutralizable. PAFS decreases, and OH– replaces $PO_4^{3-}$ in iron hydroxyphosphate and aluminum hydroxyphosphate to generate hydroxide precipitation. At this point, the adsorption of hydroxide flocs of iron and aluminum mainly removes the phosphorus at decreasing rate, resulting in coagulation [38]. This effect is undesirable as the removal rate of glyphosate and inorganic phosphorus decreases. Therefore, pH 8 is suitable.

### 3.2.3. Effect of coagulant dosage on glyphosate removal

Fig. 8a shows that the removal rate of phosphorus shows a rapid upward trend as the coagulant dosage increases, especially from 20 to 150 mg/L. At these dosages, the respective removal rates are as follows: inorganic phosphorus increases by 62.96% (29.63%–92.59%); total phosphorus increases by 58.33% (22.92%–81.25%); glyphosate increases by 52.82% (11.27%–64.08%); and organic phosphorus increases by 52.38% (14.29%–66.67%). The biological toxicity decreases. However, as the dosage continues to increase, the removal rate of inorganic phosphorus does not increase substantially. Fig. 8b shows that the biological toxicity of the solution decreases due to the increase of the above removal rates.

The results indicate that when the amount of PAFS coagulant exceeds 150 mg/L, the surface saturation of the coagulant will reach its peak, and a stable state occurs [39]. Additional PAFS in excess causes the adsorption surface of flocs to contain phosphorus substances, which have macromolecules that repel one another [40]. Therefore, considering the generation of sludge and the treatment cost, the optimal coagulant dosage is 150 mg/L.

### 3.2.4. Effect of mixing intensity on glyphosate removal

Fig. 9 shows that the removal rates steadily increase with the stirring rate. When the stirring rate is 100 rpm, the removal rates of glyphosate, total phosphorus, organic phosphorus, and inorganic phosphorus are 66.20%, 87.50%, 76.19%, and 96.30%, respectively. When the stirring rate

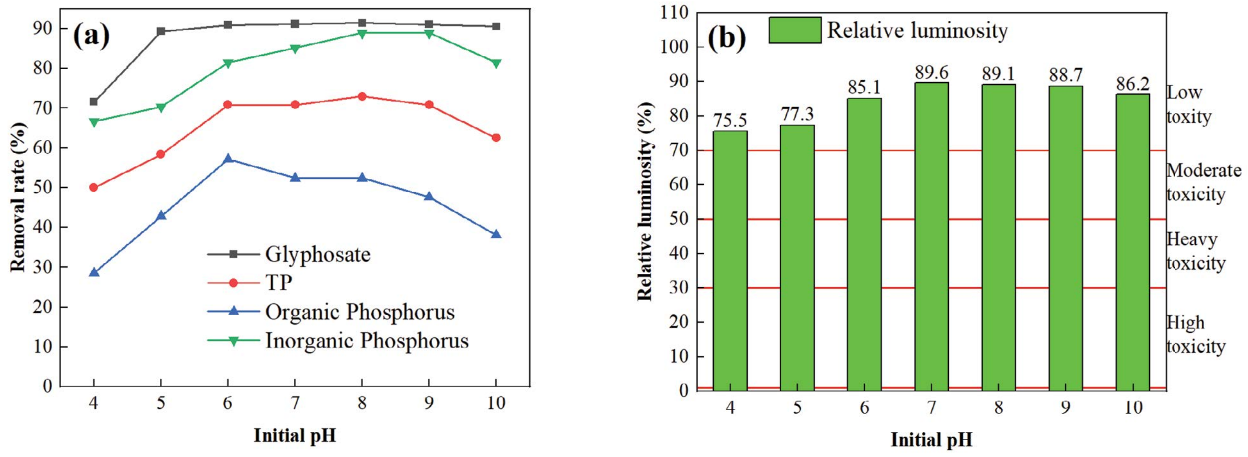

Fig. 7. Effect of pH on glyphosate removal: (a) glyphosate, total phosphorus, organic phosphorus, and inorganic phosphorus removal rates and (b) relative luminosity.

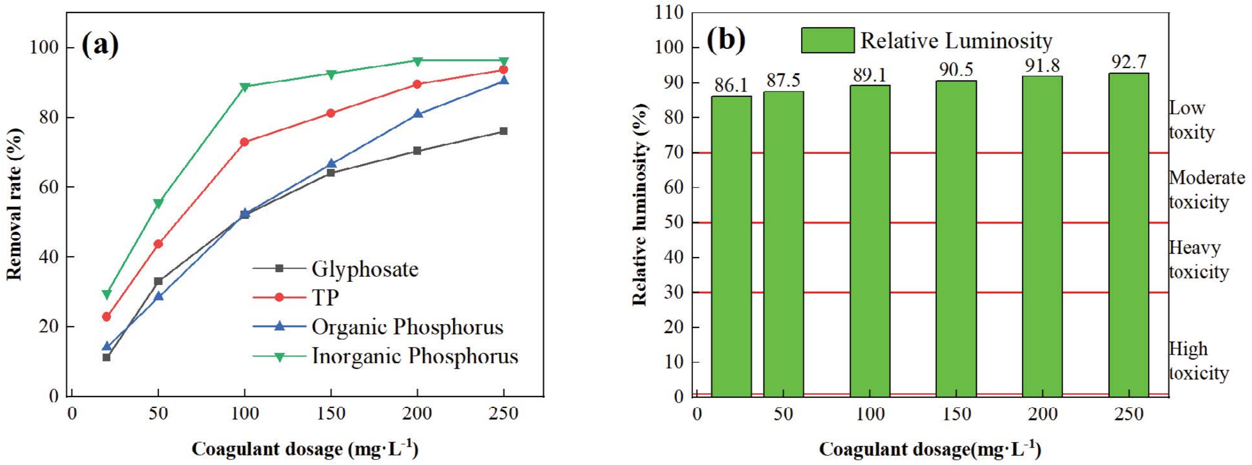

Fig. 8. Effect of coagulant dosage on glyphosate removal: (a) glyphosate, total phosphorus, organic phosphorus, and inorganic phosphorus removal rate and (b) relative luminosity.

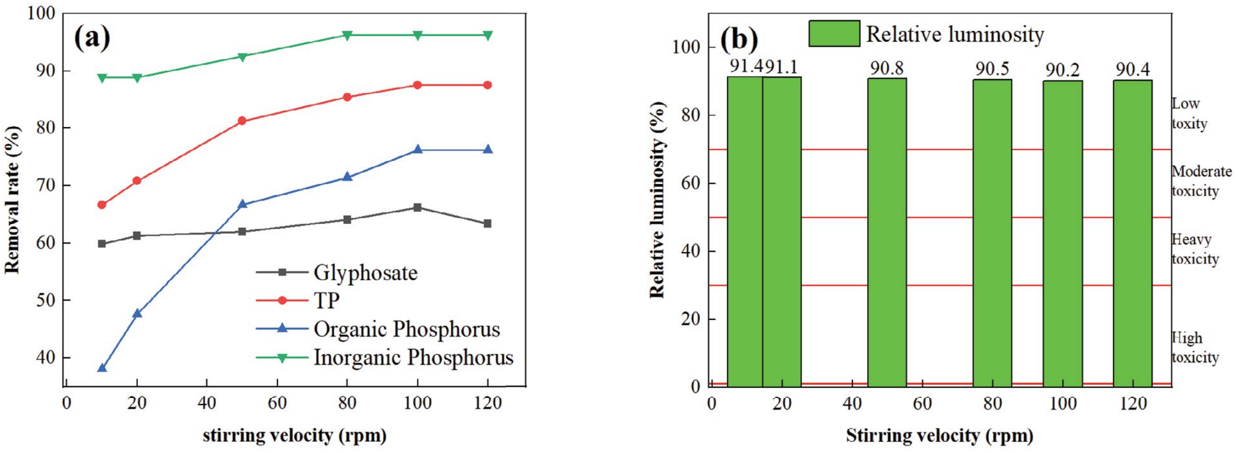

Fig. 9. Effect of mixing intensity on glyphosate removal: (a) glyphosate, total phosphorus, organic phosphorus, and inorganic phosphorus removal rates and (b) relative luminosity.

increases to 120 rpm, the removal rates remain unchanged or even decrease. Fig. 9b shows that the biological toxicity of the solution has a low correlation with changes in stirring rate.

This result may be caused by PAFS removing phosphorus-containing substances in water bodies mainly through electrical neutralization and adsorption bridging [41]. When the stirring speed is low, then PAFS cannot fully contact the phosphorus-containing substances in the sewage, and the coagulant charge and adsorption bridging decreases, resulting in poor coagulation. If the stirring speed is high, then the phosphorus-containing flocs are broken and returned to the solution due to the shearing force in the water, which weakens the adsorption bridging and net capture sweeping effect of the coagulant [42]. This state is not conducive to coagulation. Therefore, the optimal stirring rate is 100 rpm.

### *3.2.5. Effect of mixing time on glyphosate removal*

Fig. 10a shows that the removal rates of glyphosate, total phosphorus, organic phosphorus, and inorganic phosphorus initially increase and then decrease as the stirring time continues. When the stirring time is 5 min, the removal rates of glyphosate, total phosphorus, organic phosphorus, and inorganic phosphorus reach a maximum of 67.61%, 89.58%, 80.95%, and 96.30%, respectively. The relative luminescence is 90.3%, as shown in Fig. 10b.

These results are obtained because at constant stirring rate, the stirring time determines the coagulation effect. In general, lengthening the stirring time improves the treatment effect. A short stirring time causes insufficient contact between the PAFS molecules and phosphorus-containing substances, and the electrical neutralization and adsorption bridging of the coagulant decreases [43]. Lengthy stirring time destroys the formed flocs because of the shear force of the water body. The phosphorus-containing substances adsorbed by the coagulant are re-separated and released into the water body, which weakens the adsorption bridging and net capture sweeping effect of the coagulant [44]. As such, when the stirring time exceeds a certain range, the coagulant treatment efficiency decreases. Therefore, the optimum stirring time is 5 min.

### *3.2.6. Effect of wastewater temperature on glyphosate removal*

Fig. 11a shows that the removal rate of inorganic phosphorus changes slightly with the increase of reaction temperature. The removal rate is stable at approximately 95%, and the treatment effect is at its best. The removal rates of glyphosate, total phosphorus, and organic phosphorus initially increase and then decrease. At 35°C, the removal rates of glyphosate, total phosphorus, and organic phosphorus reach a maximum of 71.13%, 93.75%, and 90.48%, respectively. Fig. 11b shows that the relative luminosity of the solution reaches its maximum at 35°C, at which time the solution has the lowest toxicity.

Low water temperature may cause water viscosity to increase. Under constant stirring rate, viscosity hinders the diffusion of PAFS and sedimentation of phosphorus-containing flocs, which may affect the hydrolysis kinetic balance and the formation of metal hydroxides [45]. In addition, low-temperature results in low density of phosphorous-containing flocs, smaller flocs, and unsatisfactory coagulation effects. However, extremely high water temperature ages or decomposes PAFS into insoluble substances and reduces the coagulation effect [46]. Therefore, the preferred reaction temperature is 35°C.

### *3.3. Spectral characterization of glyphosate water*

Fig. 12 shows that glyphosate isopropylamine is highly soluble in water due to its various hydroxyl groups; thus, this substance cannot be detected by temperament extraction. After ozone-catalyzed oxidation, a large amount of alcohols are produced in the solution, which indicates that glyphosate isopropylamine releases long-chain alcohols due to the oxidative decomposition of hydroxyl and carbon chains. Ether and aldehydes shown in the figure are caused by the oxidation of carbon–oxygen double bond to a part of the ether and of the aldehyde. After oxidation, the total

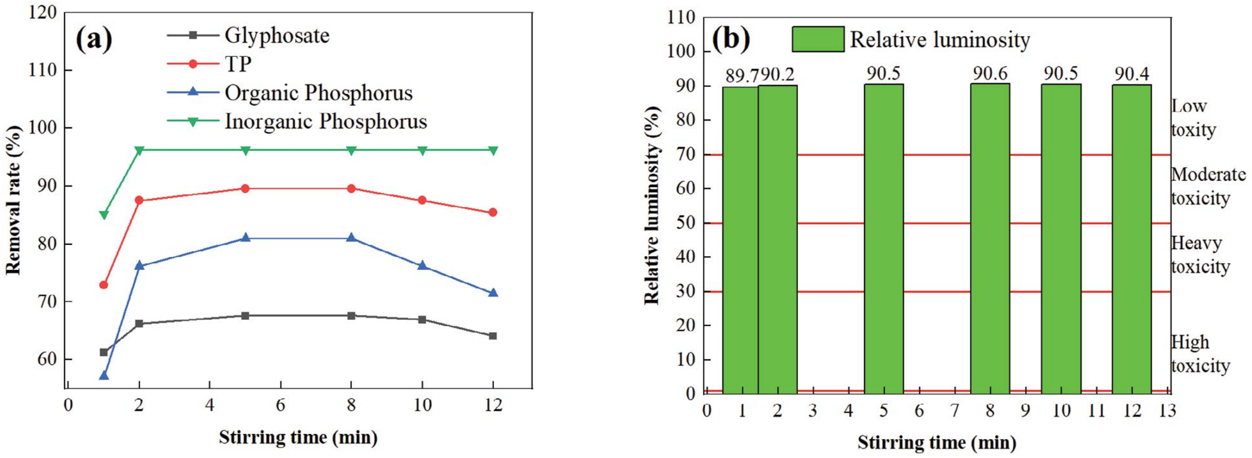

Fig. 10. Effect of mixing time on glyphosate removal: (a) glyphosate, total phosphorus, organic phosphorus, and inorganic phosphorus removal rates and (b) relative luminosity.

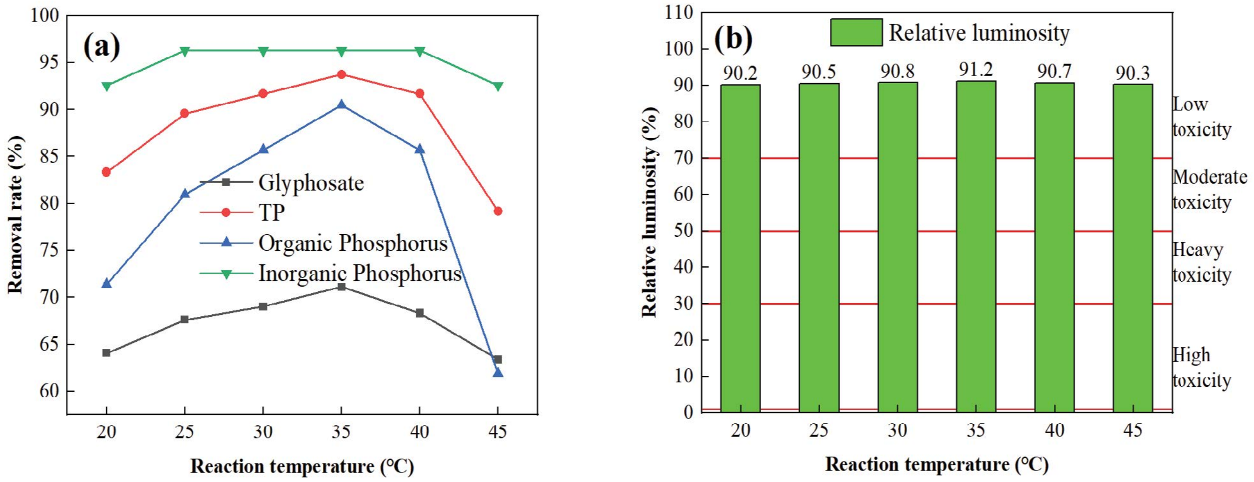

Fig. 11. Effect of wastewater temperature on glyphosate removal: (a) glyphosate, total phosphorus, organic phosphorus, and inorganic phosphorus removal rates and (b) relative luminosity.

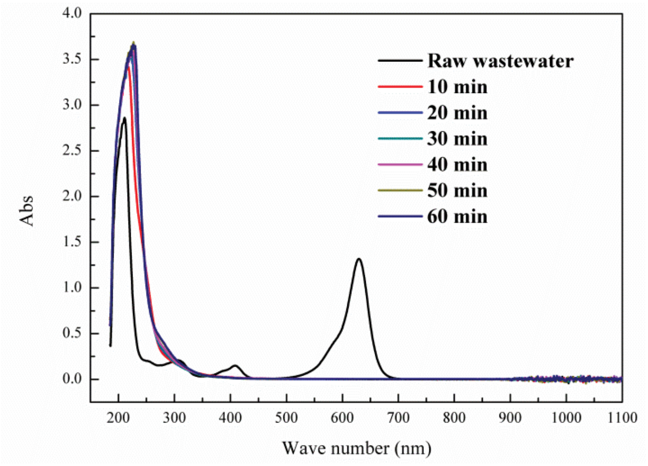

Fig. 12. Spectral characterization of glyphosate water.

phosphorus is unchanged but the inorganic phosphorus increases. This result indicates that glyphosate oxidizes to release phosphate, which increases the inorganic phosphorus content. No nitrogenous organic matter is detected in the temperament, which may cause the ammonia nitrogen in the water sample to increase after oxidation, because the nitrogenous organic matter may be converted into ammonia nitrogen or nitrate nitrogen.

According to the UV full scan, the glyphosate isopropylamine raw water has a high chroma; thus, a large absorption peak appears at 500–800 nm. After the ozone-catalytic oxidation treatment, the solution chroma removal rate increases, and color significantly decreases [47]. As the catalytic oxidation process continues, the organic phosphorus in the solution is oxidized and decomposed into inorganic phosphorus [48]. Therefore, a peak occurs at approximately 200 nm, further confirming that ozone oxidation can effectively and completely oxidize glyphosate isopropylamine.

## 4. Conclusion

In this study, ozone-catalyzed coupled coagulation is used to treat glyphosate-simulated wastewater. The experimental results show that the optimum values of ozone dosage, hydrogen peroxide, pH, reaction time, and catalyst ratio are 25 mg/L, 0.20%, 9, 20 min, and 10%, respectively, 33.4 mg/L decreases to 14.2 mg/L; and toxicity decreases from high to low. The wastewater treated under this optimal condition is then treated by coagulation and sedimentation. The single-factor experiment results show that PAFS as a coagulant achieves the most effective treatment with the highest removal rates. When the solution has pH 8, PAFS dosage of 150 mg/L, stirring rate at 100 rpm, stirring time at 2 min, and reaction temperature of 35°C, the glyphosate concentration decreases to 5.2 mg/L and the inorganic phosphorus removal rate is 96.3%. The experimental results prove that the ozone-combined coagulation and precipitation is a highly effective treatment effect for glyphosate pesticide wastewater, with short reaction time, simple treatment equipment, and easily achievable reaction conditions. Thus, the proposed process is effective for treating glyphosate wastewater.

## Acknowledgments

This research was supported by National Key Research and Development Program of China (2017YFB0602500), National Natural Science Foundation of China (No. 51508268), and 2018 Six Talent Peaks Project of Jiangsu Province (JNHB-038).

## References

[1] N. Tan, Z. Yang, X. Gong, Z. Wang, T. Fu, Y. Liu, *In situ* generation of $H_2O_2$ using MWCNT-Al/$O_2$ system and possible application for glyphosate degradation, Sci. Total Environ., 650 (2019) 2567–2576.

[2] H. Rubi-Juarez, S. Cotillas, C. Saez, P. Canizares, C. Barrera-Diaz, M.A. Rodrigo, Use of conductive diamond photo-

electrochemical oxidation for the removal of pesticide glyphosate, Sep. Purif. Technol., 167 (2016) 127–135.

[3] Y. Chang, Y. Lin, G. Xiao, T. Chiu, C. Hu, A highly selective and sensitive nanosensor for the detection of glyphosate, Talanta, 161 (2016) 94–98.

[4] M.R. Lescano, L. Pizzul, M.D.P. Castillo, C.S. Zalazar, Glyphosate and aminomethylphosphonic acid degradation in biomixtures based on alfalfa straw, wheat stubble and river waste, J. Environ. Manage., 228 (2018) 451–457.

[5] B. Xing, H. Chen, X. Zhang, Efficient degradation of organic phosphorus in glyphosate wastewater by catalytic wet oxidation using modified activated carbon as a catalyst, Environ. Technol., 39 (2018) 749–758.

[6] M.P. Rosa Barbosa, N.S. Lima, D.B. de Matos, R.J. Alves Felisardo, G.N. Santos, G.R. Salazar-Banda, E.B. Cavalcanti, Degradation of pesticide mixture by electro-Fenton in filter-press reactor, J. Water Process Eng., 25 (2018) 222–235.

[7] E. Rott, T. Pittmann, S. Wasielewski, A. Kugele, R. Minke, Detoxification of pesticide-containing wastewater with Fe-III, activated carbon and Fenton reagent and its control using three standardized bacterial inhibition tests, Water, 9 (2017) 969, doi: 10.3390/w9120969.

[8] Q. Yang, J. Wang, X. Chen, W. Yang, H. Pei, N. Hu, Z. Li, Y. Suo, T. Li, J. Wang, The simultaneous detection and removal of organophosphorus pesticides by a novel Zr-MOF based smart adsorbent, J. Mater. Chem. A, 6 (2018) 2184–2192.

[9] S. Fiorilli, L. Rivoira, G. Cali, M. Appendini, M.C. Bruzzoniti, M. Coisson, B. Onida, Iron oxide inside SBA-15 modified with amino groups as reusable adsorbent for highly efficient removal of glyphosate from water, Appl. Surf. Sci., 411 (2017) 457–465.

[10] B. Xing, H. Chen, X. Zhang, Removal of organic phosphorus and formaldehyde in glyphosate wastewater by CWO and the lime-catalyzed formose reaction, Water Sci. Technol., 75 (2017) 1390–1398.

[11] M. Ahmadib, F. Ghanbari, Degradation of organic pollutants by photoelectro-peroxone/ZVI process: synergistic, kinetic and feasibility studies, J. Environ. Manage., 228 (2018) 32–39.

[12] P. Frangos, H. Wang, W. Shen, G. Yu, S. Deng, J. Huang, B. Wang, Y. Wang, A novel photoelectro-peroxone process for the degradation and mineralization of substituted benzenes in water, Chem. Eng. J., 286 (2016) 239–248.

[13] B. Liu, S. Pan, Z. Liu, X. Li, X. Zhang, Y. Xu, Y. Sun, Y. Yu, H. Zheng, Efficient removal of Cu(II) organic complexes by polymer-supported, nanosized, and hydrated Fe(III) oxides through a Fenton-like process, J. Hazard. Mater., 386 (2019) 121969, doi: 10.1016/j.jhazmat.2019.121969.

[14] Y. Li, C. Zhao, Y. Wen, Y. Wang, Y. Yang, Adsorption performance and mechanism of magnetic reduced graphene oxide in glyphosate contaminated water, Environ. Sci. Pollut. Res., 25 (2018) 21036–21048.

[15] H. Zheng, Y. Sun, C. Zhu, J. Guo, C. Zhao, Y. Liao, Q. Guan, UV-initiated polymerization of hydrophobically associating cationic flocculants: synthesis, characterization, and dewatering properties, Chem. Eng. J., 234 (2013) 318–326.

[16] L. Heritier, A. Meistertzheim, O. Verneau, Oxidative stress biomarkers in the Mediterranean pond turtle (*Mauremys leprosa*) reveal contrasted aquatic environments in Southern France, Chemosphere, 183 (2017) 332–338.

[17] W. Sun, Y. Sun, H. Zhu, H. Zheng, Catalytic activity and evaluation of Fe-Mn@Bt for ozonizing coal chemical biochemical tail water, Sep. Purif. Technol., 239 (2020) 116524, doi: 10.1016/j.seppur.2020.116524.

[18] T. Poiger, I.J. Buerge, A. Bachli, M.D. Muller, M.E. Balmer, Occurrence of the herbicide glyphosate and its metabolite AMPA in surface waters in Switzerland determined with on-line solid phase extraction LC-MS/MS, Environ. Sci. Pollut. Res., 24 (2017) 1588–1596.

[19] Z. Xiong, B. Lai, P. Yang, Insight into a highly efficient electrolysis-ozone process for N,N-dimethylacetamide degradation: quantitative analysis of the role of catalytic ozonation, Fenton-like and peroxone reactions, Water Res., 140 (2018) 12–23.

[22] B. Xu, Q. Sun, J.C. Lan, W. Chen, C. Hsueh, B. Chen, Exploring the glyphosate-degrading characteristics of a newly isolated, highly adapted indigenous bacterial strain, Providencia rettgeri GDB 1, J. Biosci. Bioeng., 128 (2019) 80–87.

[23] Q. Chen, J. Zheng, Q. Yang, Z. Dang, L. Zhang, Insights into the glyphosate adsorption behavior and mechanism by a MnFe$_2$O$_4$@ cellulose-activated carbon magnetic hybrid, ACS Appl. Mater. Interfaces, 11 (2019) 15478–15488.

[24] S. Sun, S. Wang, Y. Ye, B. Pan, Highly efficient removal of phosphonates from water by a combined Fe(III)/UV/co-precipitation process, Water Res., 153 (2019) 21–28.

[25] Y. Yang, Q. Deng, Y. Zhang, Comparative study of low-index {101}-TiO$_2$, {001}-TiO$_2$, {100}-TiO$_2$ and high-index {201}-TiO$_2$ on glyphosate adsorption and photo-degradation, Chem. Eng. J., 360 (2019) 1247–1254.

[26] M. Muruganandham, M. Swaminathan, Decolourisation of Reactive Orange 4 by Fenton and photo-Fenton oxidation technology, Dyes Pigm., 63 (2004) 315–321.

[27] M.A. Zazouli, F. Ghanbari, M. Yousefi, S. Madihi-Bidgoli, Photocatalytic degradation of food dye by Fe$_3$O$_4$–TiO$_2$ nanoparticles in presence of peroxymonosulfate: the effect of UV sources, J. Environ. Chem. Eng., 5 (2017) 2459–2468.

[28] N. Jaafarzadeh, F. Ghanbari, M. Moradi, Photo-electro-oxidation assisted peroxymonosulfate for decolorization of acid brown 14 from aqueous solution, Korean J. Chem. Eng., 32 (2015) 458–464.

[29] Z. Xiong, J. Cao, D. Yang, B. Lai, P. Yang, Coagulation–flocculation as pre-treatment for micro-scale Fe/Cu/O$_3$ process (CF-mFe/Cu/O$_3$) treatment of the coating wastewater from automobile manufacturing, Chemosphere, 166 (2017) 343–351.

[30] Z. Xiong, B. Lai, Y. Yuan, J. Cao, P. Yang Y. Zhou, Degradation of p-nitrophenol (PNP) in aqueous solution by a micro-size Fe$^0$/O$_3$ process (mFe$^0$/O$_3$): optimization, kinetic, performance and mechanism, Chem. Eng. J., 302 (2016) 137–145.

[31] D. Jia, M. Liu, J. Xia, C. Li, Effective removal of aqueous glyphosate using CuFe$_2$O$_4$@biochar derived from phragmites, J. Chem. Technol. Biotechnol., 95 (2020) 196–204.

[32] B. Mathon, M. Coquery, C. Miege, A. Vandycke, J.M. Choubert, Influence of water depth and season on the photodegradation of micropollutants in a free-water surface constructed wetland receiving treated wastewater, Chemosphere, 235 (2019) 260–270.

[33] L. Cao, D. Ma, Z. Zhou, C. Xu, C. Cao, P. Zhao, Q. Huang, Efficient photocatalytic degradation of herbicide glyphosate in water by magnetically separable and recyclable BiOBr/Fe$_3$O$_4$ nanocomposites under visible light irradiation, Chem. Eng. J., 368 (2019) 212–222.

[34] H. Zheng, Y. Sun, J. Guo, F. Lo, W. Fan, Y. Liao, Q. Guan, Characterization and evaluation of dewatering properties of PADB, a highly efficient cationic flocculant, Ind. Eng. Chem. Res., 53 (2014) 2572–2582.

[35] Y. Sun, M. Ren, C. Zhu, Y. Xu, H. Zheng, X. Xiao, H. Wu, T. Xia, Z. You, UV-initiated graft copolymerization of cationic chitosan-based flocculants for treatment of zinc phosphate-contaminated wastewater, Ind. Eng. Chem. Res., 55 (2016) 10025–10035.

[36] Y. Sun, C. Zhu, H. Zheng, W. Sun, Y. Xu, X. Xiao, Z. You, C. Liu, Characterization and coagulation behavior of polymeric aluminum ferric silicate for high-concentration oily wastewater treatment, Chem. Eng. Res. Des., 119 (2017) 23–32.

[37] W. Sun, G. Ma, Y. Sun, Y. Liu, N. Song, Y. Xu, H. Zheng, Effective treatment of high phosphorus pharmaceutical wastewater by chemical precipitation, Can. J. Chem. Eng., 95 (2017) 1585–1593.

[38] M. Tang, Y. Sun, C. Zhu, Y. Xu, H. Zheng, X. Xiao, W. Sun, H. Wu, C. Liu, Preparation of polymeric aluminum ferric silicate for the pre-treatment of oily wastewater through response surface method, Desal. Water Treat., 65 (2017) 284–293.

[39] Y. Sun, S. Zhou, S. Pan, S. Zhu, Y. Yu, H. Zheng, Performance evaluation and optimization of flocculation process for removing heavy metal, Chem. Eng. J., 385 (2020) 123911, doi: 10.1016/j.cej.2019.123911.

[40] Y. Sun, C. Zhu, W. Sun, Y. Xu, X. Xiao, H. Zheng, H. Wu, C. Liu, Plasma-initiated polymerization of chitosan-based

CS-g-P(AM-DMDAAC) flocculant for the enhanced flocculation of low-algal-turbidity water, Carbohydr. Polym., 164 (2017) 222–232.

[41] Y. Sun, W. Sun, K.J. Shah, P. Chiang, H. Zheng, Characterization and flocculation evaluation of a novel carboxylated chitosan modified flocculant by UV initiated polymerization, Carbohydr. Polym., 208 (2019) 213–220.

[42] Y. Sun, K.J. Shah, W. Sun, H. Zheng, Performance evaluation of chitosan-based flocculants with good pH resistance and high heavy metals removal capacity, Sep. Purif. Technol., 215 (2019) 208–216.

[43] Y. Sun, A. Chen, S. Pan, W. Sun, C. Zhu, K.J. Shah, H. Zheng, Novel chitosan-based flocculants for chromium and nickel removal in wastewater via integrated chelation and flocculation, J. Environ. Manage., 248 (2019), doi: 10.1016/j.jenvman.2019.07.012.

[44] L. Chen, Y. Sun, W. Sun, K.J. Shah, Y. Xu, H. Zheng, Efficient cationic flocculant MHCS-g-P(AM-DAC) synthesized by UV-induced polymerization for algae removal, Sep. Purif. Technol., 210 (2019) 10–19.

[45] Z. You, C. Zhuang, Y. Sun, S. Zhang, H. Zheng, Efficient removal of $TiO_2$ nanoparticles by enhanced flocculation–coagulation, Ind. Eng. Chem. Res., 58 (2019) 14528–14537.

[46] L. Chen, H. Zhu, Y.J. Sun, P.C. Chiang, W.Q. Sun, Y.H. Xu, H.L. Zheng, K.J. Shah, Characterization and sludge dewatering performance evaluation of the photo-initiated cationic flocculant PDD, J. Taiwan Inst. Chem. Eng., 93 (2018) 253–262.

[47] C. Soares, R. Pereira, S. Spormann, F. Fidalgo, Is soil contamination by a glyphosate commercial formulation truly harmless to non-target plants? - Evaluation of oxidative damage and antioxidant responses in tomato, Environ. Pollut., 247 (2019) 256–265.

[48] D.Y. Yushchenko, P.A. Simonov, T.B. Khlebnikova, Z.P. Pai, V.I. Bukhtiyarov, Oxidation of N-isopropyl phosphonomethyl glycine with hydrogen peroxide catalyzed by carbon-supported gold nanoparticles, Catal. Commun., 121 (2019) 57–61.